# Amass

## Advanced manufacturing for the assembly of structural steel

Shemshadian, Mohammad E.; Schultz, Arturo E.; Le, Jia Liang; Labbane, Ramzi; Laefer, Debra F.; Al-Sabah, Salam; Truong-Hong, Linh; Huynh, Minh Phuoc; McGetrick, Patrick; Martin, Tony

**DOI**
10.1061/(ASCE)SC.1943-5576.0000516

**Publication date**
2021

**Document Version**
Accepted author manuscript

**Published in**
Practice Periodical on Structural Design and Construction

# AMASS: Advanced Manufacturing for the Assembly of Structural Steel

Mohammad E. Shemshadian[1], Arturo Schultz[1], Jia-Liang Le[1], Ramzi Labbane[1], Debra Laefer[2,3], Salam Al-Sabah[3], Linh Truong-Hong[4], Minh Huynh[3], Patrick McGetrick[5], Tony Martin[5], and Pantelis Matis[5]

[1]*Department of Civil, Environmental and Geo- Engineering, University of Minnesota, Twin Cities, USA*

[2]*Center for Urban Science and Progress and Department of Civil and Urban Engineering, Tandon School of Engineering, New York University, New York, USA*

[3]*School of Civil Engineering, University College Dublin, Dublin, Ireland*

[4]*Dept. of Geoscience and Remote Sensing, Delft Univ. of Technology, 2628 CN Delft, Netherlands*

[5]*School of Natural and Built Environment, Queen's University Belfast, Belfast, Northern Ireland*

## Abstract

This paper describes a collaborative project between researchers in the US, Ireland, and Northern Ireland (UK) to investigate advanced manufacturing techniques for the creation of a new class of 'intermeshed steel connections' that rely on neither welding nor bolting. To date, advanced manufacturing equipment has only been used to accelerate traditional processes for cutting sheet metal or other conventional fabrication activities. Such approaches have not capitalized on the equipment's full potential. This project lays the groundwork to transform the steel building construction industry by investigating the underlying science and engineering precepts for intermeshed connections created from precise, volumetric cutting. The proposed system enhances the integration between design, fabrication, installation, and maintenance. Fully automated, precise, volumetric cutting of open steel sections introduces intellectual challenges regarding the

load-transfer mechanisms and failure modes for intermeshed connections. The research activity addresses knowledge gaps concerning the load resistance and design of steel systems with intermeshed connections. Physical tests and finite element modeling were used to investigate the mechanics of intermeshed connections including stress and strain concentrations, fracture potential and failure modes, and to optimize connection geometry.

**Keywords:** Steel Connection, Intermeshed, Plasma, Waterjet, Finite Element Modeling, Experiment.

## 1. INTRODUCTION

Despite field welding and bolting being time-consuming and/or expensive, the steel building market has not developed any new universally applicable structural steel connection systems since before World War II. To achieve improved construction efficiency and heightened material reuse, computer controlled, advanced manufacturing techniques in high-definition plasma, laser and waterjet cutting could be exploited [1]. This paper envisions the harnessing of those technologies to create an entirely new class of "intermeshed" steel connections.

Precise cutting of steel makes it possible to create the notches in beam flanges and web that can intermesh with other beam parts or external connectors, like puzzle pieces. This technique could radically change how structural steel is fabricated, assembled, deconstructed, and reused [2]. Without relying solely on bolting or welding to assemble a connection in the field, the simplicity and efficiency of the construction process may be significantly improved. To date, this class of fabrication equipment has only been used to accelerate traditional processes for cutting sheet metal

or other conventional fabrication activities (e.g. cutting instead of drilling holes). Such approaches have not capitalized on the equipment's full potential.

Because assembly and inspections costs at a construction site are high for welded and bolted connections, the intermeshed connection offers the potential for a lower cost connection, even though manufacturing costs are likely to be higher. There is also the potential for life cycle savings as deconstruction costs would be significantly lower as an intermeshed connection can be designed specifically for disassembly and reuse. However, unlike traditional bolted or welded connections, where the industry has more than 100 years of experience, precise cutting of steel for an intermeshed connection is not yet part of the culture or expectations.

While maintaining the original concept, different details can be proposed for the intermeshed connection. In this paper, two variations of the intermeshed connection are presented and studied in the following sections.

## 2. AUTOMATION IN STEEL CONSTRUCTION

Construction is one of the largest sectors in the world economy and approximately 7% of the world working population is employed by construction-related services. However, the productivity of this industry has barely grown for decades compared to other industries. Since 1945 in the United States, the overall productivity in all sectors has grown by 400 percent, while productivity in construction has not increased at all (Fig. 1) [3]. One of the reasons for this underperformance is that the construction industry is highly regulated, and the common techniques have not been updated in years. Steel construction as a subcategory of the construction sector has also suffered from restrictive design specifications, underinvestment in skills development, and

insufficient innovation. Consequently, commonly used alternatives for steel connections have not been developed in the past 50 years.

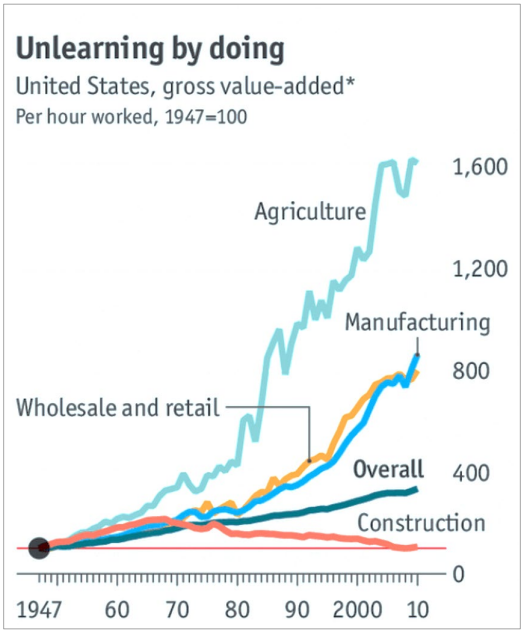


Fig. 1: Productivity of different sectors in United States [3]

Developing new construction methodologies such as prefabricated volumetric construction and digital technologies can further facilitate off-site fabrication. Specifically, in the steel construction industry, 'advanced manufacturing techniques' such as plasma cutting and waterjet cutting could be utilized. These fully automated cutting techniques could enhance the fabrication process and consequently increase construction productivity.

Traditionally, steel plates are cut using saws or oxy-fuel for structural purposes. These techniques are mainly applied manually, which results in highly variable speed and accuracy. The new computer-controlled cutting techniques would help improve the precision of fabrication, and by combining them with robotic arms, faster and more flexible operation would ensue. Although

a variety of options is available based on project needs, this research focuses on the implementation of plasma and waterjet cutting in steel fabrication.

High definition plasma cutting is a thermal process achieved through a concentrated high-speed plasma stream [4]. The plasma stream is extremely hot at up to 30,000 K, and it cuts through the material by melting it [5]. The plasma cutter may be attached to a robotic arm with multiple degrees of freedom, giving it unlimited possibilities regarding the position and configuration of the cut surfaces. Waterjet cutting can also be used to precisely cut various materials, including structural steel. High pressure waterjets with abrasive additives are used to cut the material by eroding away at the surface [4]. This form of cutting may be a desirable alternative to plasma cutting due to its lower energy demand and lack of thermal effects on the cut material [6]. Moreover, waterjet provides more precise cuts in a wider range of plate thickness. As an emerging technology with certain advantages over other cutting methods, use of waterjet cutting may become more widespread in the future.

Using these cutting techniques can open up an opportunity to create an alternative steel connection that relies on intermeshed (i.e. interlocked) components, instead of regular welding or bolting techniques. In this class of connection, the force transfer is achieved through direct contact bearing of multiple, precisely shaped surfaces of the interlocking elements. However, due to the absence of welds or bolts in the connection detail, it is likely that the intermeshed connection would not behave as a fully rigid connection. Therefore, the effects of implementing such connections needs to be evaluated by investigating the response of steel frames equipped with intermeshed connections.

# 3. MOMENT FRAMES WITH INTERMESHED CONNECTION

Structural connections are frequently assumed as ideally pinned or fixed in numerical modeling. However, these assumptions do not accurately represent the behavior of the intermeshed connection. In reality, the connection stiffness is expected to be somewhere between the two extremes due to the cuts in section which causes discontinuity in the load path. Therefore, in the case of this connection, a spring with assigned stiffness is more representative and helps achieve reasonable accuracy in the frame responses. However, inclusion of the connection stiffness in the analysis affects the distribution of the internal forces and deformations in the frame and needs further investigation. To determine the influence of connection rigidity on frame response, a series of linear analyses was conducted on variety of frames with different connection properties. The goal is to understand the influence of connection rigidity on frame overall stiffness as well as stress distribution in different frame members. At the end of this step, practical recommendations will be provided on 'optimal locations' and 'suitable stiffness range' for the intermeshed connection.

Members and connections in gravity framing are typically designed to resist vertical loads. However, most building structures are subjected to lateral loads with wind and seismic forces being the most common. Even though lateral load resisting systems such as structural cores and braced frames are often used to resist these loads, the gravity frames must undergo the associated lateral displacements with little or no loss in vertical load capacity. This ability can be quantified by determining the changes in internal forces (moment, shear, and axial forces) that occur under the imposed lateral drifts. Large increases in these internal forces would be indicative of gravity framing that would be at risk.

This aspect of the research utilized two-dimensional (2D) pushover analysis with commercial software SAP2000. Translational ($K_1$, $K2$) and rotational ($K_3$) stiffness of the intermeshed connection were idealized as elastic springs in linear elastic models of prototype steel frames and the models were analyzed under various load schemes. First, gravity (dead and live) load was applied, and then, the frames were pushed to 2% of their height to simulate the maximum expected drift from the lateral force. A range of 2D frames with different geometries for 3-story and 9-story frames, with span-to-height ratio of two and three, were considered. Changes in internal forces are affected by the location and stiffness of the spring. Therefore, to find the optimal location of the connection, the position of the connections ($a$) in the span length ($L$) was changed from zero to 0.25 of $L$ gradually (i.e., $a/L$= 0, 0.05, 0.1, 0.15, 0.2, and 0.25). Since the detail of the connection had not been defined at this stage, the translational and rotational stiffness coefficients of the connection were unknown. Therefore, a wide range of spring stiffness was assumed: 20, 10, 5, 1, 0.5, 0.2, and 0.1 times of the beam stiffness, which were defined for the three structural actions as follows. Axial stiffness ($EA/L$), shear stiffness ($GA/L$), and flexural stiffness ($EI/L$) were calculated using geometric properties of the beam section ($A$ and $I$), beam length ($L$), and elastic material properties of the structural steel ($E$ and $G$). To fully cover the range of selected variables in frames, more than 300 frames were modeled and analyzed.

Rotational stiffness of the connection, $K_3$, was found to affect frame lateral stiffness (Fig. 2) and beam deflection drastically, especially when the connections are located near the beam ends. According to AISC recommendations, the minimum value for rotational stiffness of a connection to be categorized as fully rigid is 20 ($K_3 \geq 20EI/L$). Fig. 2 also shows that beyond the same stiffness limit, increasing rotational stiffness produces no appreciable change in structural response, regardless of the connection location. Considering $K_3 \geq 20EI/L$ (i.e. fully rigid frame) to be the

benchmark case, comparison could be performed to learn the effect of reduction in the connection rotational stiffness on the fundamental period of the frame. Fig. 2 shows changes in the frame fundamental period based on changes in the ratio of connection rotational stiffness to beam flexural stiffness ($K_3 / (EI/L)$). It can be seen that although a reduction of this ratio below 20 increases the fundamental period of the frame, the increases are limited to a range of 10% to 20%, even when the ratio drops to 10 and 5 respectively. This is a promising discovery, since connection rotational stiffness values of *5EI/L* to *10EI/L* in the intermeshed connection may be possible without requiring a cumbersome geometry.

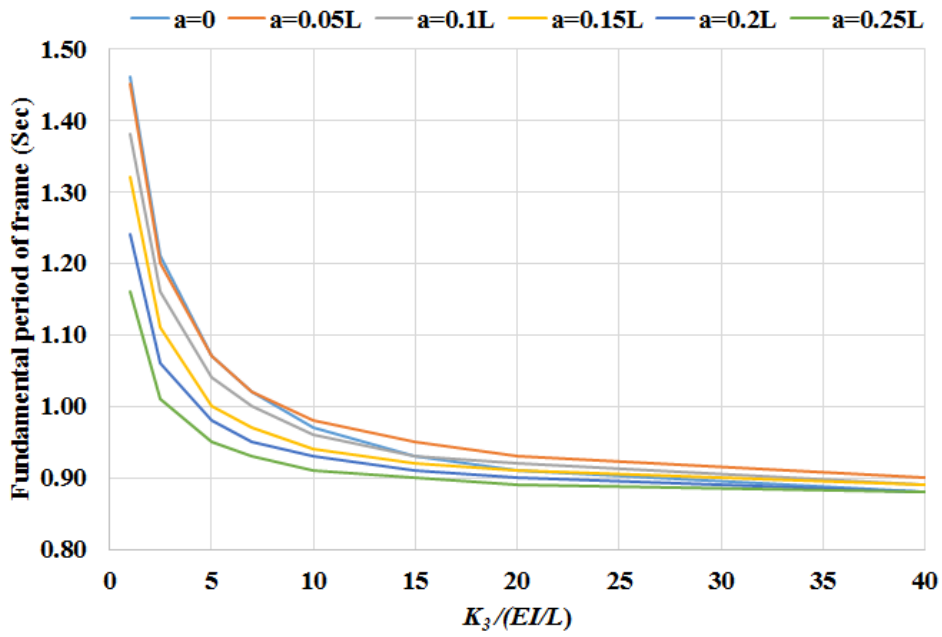


Fig. 2: Effects of connection rotational stiffness ($K_3$) and connection location (a) on fundamental period of the frame

As previously defined, a benchmark case is a frame in which all the connections are fully rigid and located at beam ends, and all the beams and columns are continuous. Variant frame cases

consist of new connection locations and/or new connection rotational stiffness values, but the same beams and columns section sizes. In the next stage of frame analysis, the maximum *P-M* (axial load combined with moment) stress ratio in each frame was calculated based on the following equation:

$$\text{Stress ratio} = \frac{P_r}{P_a} + \frac{M_r}{M_a}$$

Where $P_r$ and $M_r$ are required axial and flexural strength, and $P_a$ and $M_a$ are available axial and flexural strength respectively. Fig. 3 shows that the optimum stress ratio exists at a smaller stiffness ratio, when the connection was located closer to the beam ends. Therefore, it is easier to control the stress ratios of the beam, as the connection is located closer to the beam ends. The optimal location of the connection was defined at *0.1L* from the beam ends. Having the connection at this location led to smaller beam stress ratios for a wider range of stiffness ratio, which is a result of a more uniform moment distribution in the beam length. It also needs to be mentioned that the obtained ration (*0.1L*) is compatible with the current codes recommendations for the plastic hinge length. Table 1 shows the frame responses when the intermeshed connection was placed at *0.1L* from the span ends. Selecting a connection rotational stiffness of *5EI/L* or *10EI/L* (or any value in between), would result in reduction in the frame *P-M* stress ratios while the fundamental period undergoes a slight increase, which means the frame lateral stiffness is not dropping significantly.

Table 1: Change of the frame responses when *a=0.1L*

| ***K₃*** | ***2EI/L*** | ***5EI/L*** | ***10EI/L*** |
|---|---|---|---|
| Reduction in *P-M* stress ratios | 25% | 23% | 16% |

| | | | |
|---|---|---|---|
| Increase in fundamental period of frame | 35% | 16% | 7% |

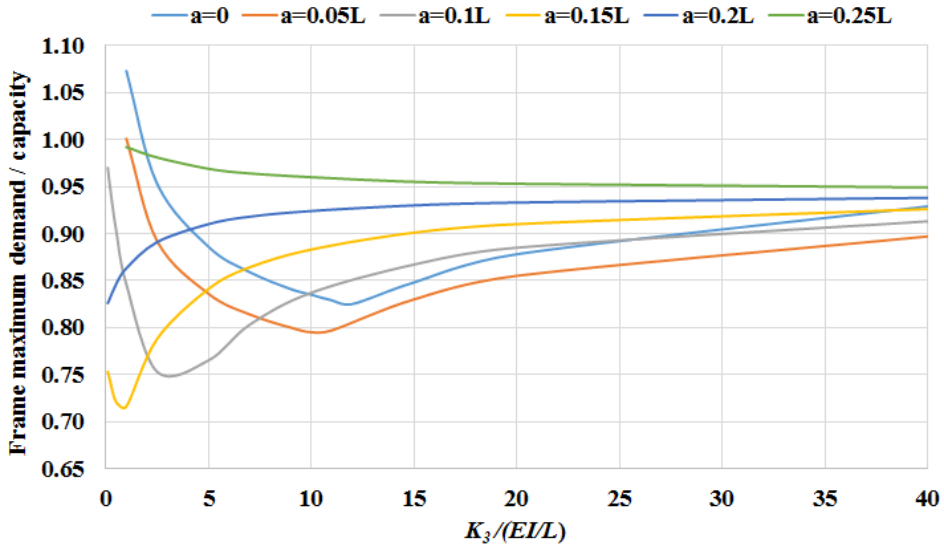


Fig. 3: Effects of connection rotational stiffness ($K_3$) and connection location (a) on beam stress ratio

## 4. FRONT-INTERMESHED CONNECTION

The first conception was a relatively simple intermeshed connection denoted as the "Front-Intermeshed Connection" [7]. This connection is composed of three-dimensional interlocking through the top and bottom flanges and through the web. The flanges carry the tension and compression resulting from the bending moment at the connection while the web carries the shear force. The connection transfers shear and compression from one beam section to the next through direct contact bearing of multiple, precisely shaped faces (Fig. 4a). The arrangement is ideally suited for connecting beams at or near ideal inflections points to create gravity load framings. For

practical use of this new type of connection, understanding its mechanical behavior, especially in terms of the load carrying capacity under mixed mode loading scenarios is essential.

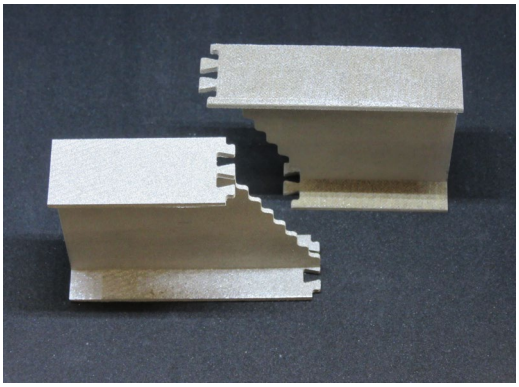

(a) Idealized connection in printed stainless steel

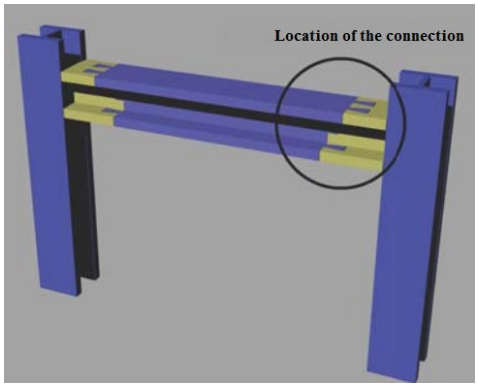


(b) Assembly of the connection in a frame

Fig. 4: Front-intermeshed connection

Load is transferred between flanges through bearing and friction via the intermeshed dovetails of the flanges. The connection has the advantage of simplicity and requires no additional parts to create the flange connection, although a locking mechanism can be added to provide resistance against uplift. However, field-assembled locking connections are unlikely to be able to fully transmit the flexural, axial and shear capacities of the connected steel sections and may reduce the corresponding stiffness components of a continuous steel member, due to interruptions in the load path.

The stepped web connection allows for easy site assembly, as the middle beam part can be dropped from above, in a method similar to current practice. In Fig. 4b, the ends shown in yellow are shop welded as stubs to the column. No other welding is required, and bolting is fully avoided in this configuration. The main drawbacks to this type of connection are the tightness of the tolerances and the lack of adjustability in the erection process.

209 To better understand how this type of precise interlocking performs structurally, initial
210 laboratory testing was conducted for the two-dimension meshed “dovetails” [8]. Based on the
211 success of those initial tests, a three-dimensional numerical model was created in Abaqus [9].
212 Finite element analyses were performed under different load combinations to investigate the
213 general behavior, failure modes, and peak capacity of the connection. Under flexure, the
214 connection shows a uniformly monotonic behavior with a relatively low flexural resistance. Failure
215 occurs when the dovetails on one side of the top flange slip out of the sockets on the other side
216 (Fig. 5a), so there is no capacity to carry tension force, which means no moment capacity can be
217 developed. Moreover, in the case of combined tension and shear, the presence of the shear force
218 causes relative vertical movement between the two sides of the connection and, consequently, the
219 flanges slip out of their intermeshed positions. When this phenomenon happens (Fig. 5b), there is
220 no component to resist tension, and the connection fails.

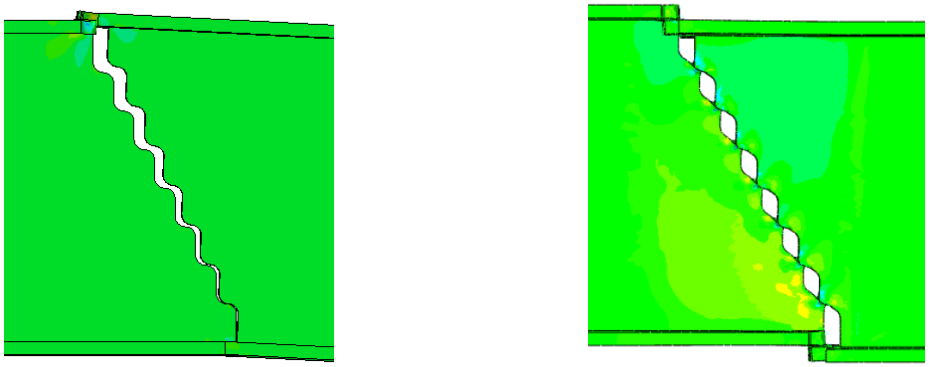

(a) In pure flexure, top flange slips out

(b) In combined tension and shear, top and bottom flanges slip out

221 Fig. 5: Performance of the front-intermeshed connection under different load conditions

222

223 Considering the connection configuration and the results of the finite element analyses, the
224 front-intermeshed connection cannot generate sufficient strength and stiffness for effective use in
225 practice. Following current code standards and based on the results from the finite element studies,

the front-intermeshed connection shows limited stiffness, strength, and ductility. So, it is classified as a non-ductile and partially restrained connection [10,11]. This classification is due to the cuts in the flanges which reduce load carrying capacity in tension and, consequently, the moment significantly. Therefore, the front-intermeshed connection is not recommended for use where demands for 1) large moments, 2) large moments in combination with large shears, and 3) axial tension are possible.

## 5. SIDE-INTERMESHED CONNECTION

Given the limitations of the front-intermeshed connection in transferring loads, especially when combined loads are present, and the requirement for strict tolerances, another alternative of the intermeshed connection is proposed [12]. The "Side-Intermeshed Connection" employs intermeshed external connectors to transfer flanges tension and compression forces.

At this step, two different versions of side-intermeshed connection were developed. The 'original conception' (Fig. 6) sought to meet the original goals of requiring no welding nor bolting, while maximizing erection speed and construction tolerance. Meanwhile, the modified version (Fig. 7) was developed for greater acceptance in the construction industry. The remainder of the paper focuses on the modified side-intermeshed connection.

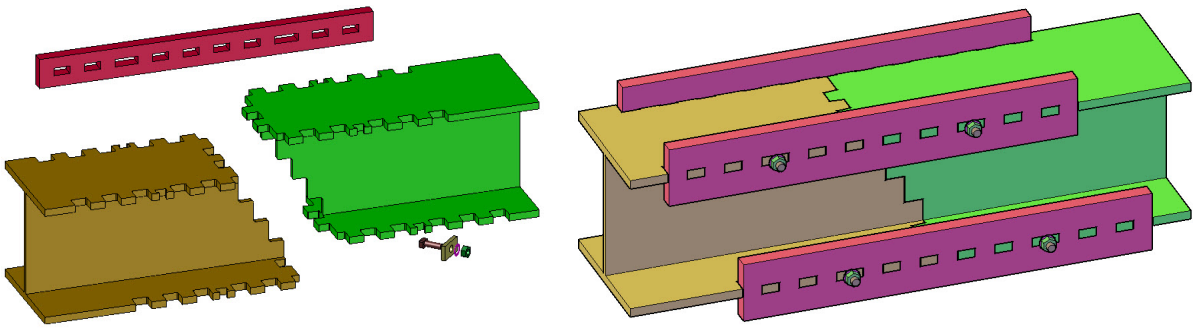

(a) 3D Exploded view (b) 3D View of assembled connection

Fig. 6: Side-intermeshed connection (original conception)

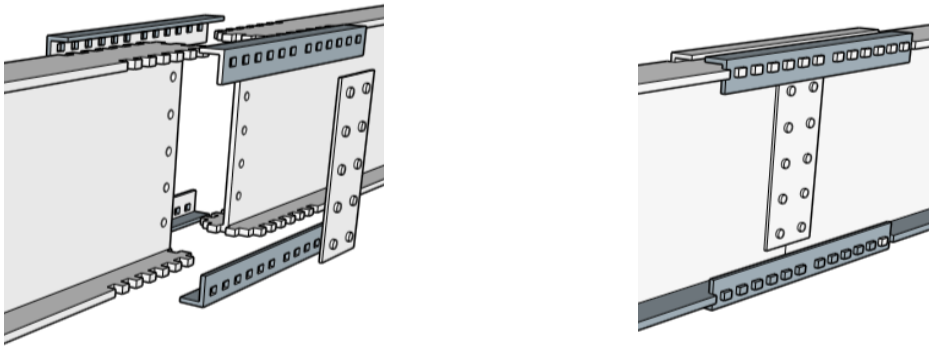

(a) 3D Exploded view (b) 3D View of assembled connection

Fig. 7: Side-intermeshed connection (modified version)

In this connection, flange edges are cut to create a set of tooth-shape notches (i.e. 'teeth'). To connect different sides of the beam, an angle is used on each edge with rectangular holes (sockets) which match the teeth (see Fig. 7). Having the beam flanges connected, the section will be able to transfer moments via the connector angles. However, for shear transfer, a pair of regular shear plates are bolted to the beam web.

The side-intermeshed connection allows larger tolerances and easier fabrication, which leads to a better potential for wider acceptance in practice. However, one potential concern related to this connection is the stress concentration at the sharp corners of the angle sockets. Depending

on the length-to-width ratio of the angle sockets, previous studies have shown that the stress concentration factor can be up to five [13] which can result in a pre-mature rupture. To avoid any undesirable failure modes, circular holes were added to the sharp corners in the angle sockets. A finite element model proved the effectiveness of such a change by reducing the stress concentration factor to 1.7. Fig. 8 shows the configuration of the socket and the resulting stress.

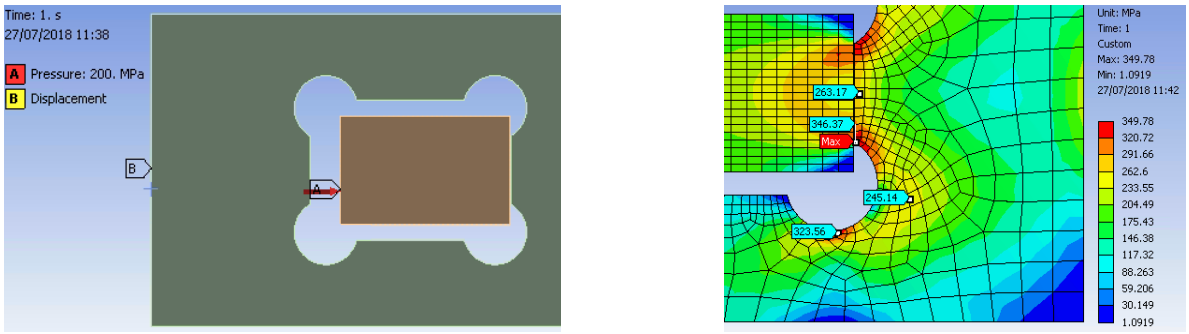


(a) Load and boundary conditions (b) Equivalent stress around the corner

Fig. 8: Finite element analysis on the effect of the shape on the stress concentration around the socket

### 5.1. Design procedure and analysis method

A procedure was developed for analyzing and designing the modified side-intermeshed connection (Fig. 7) using fundamentals of structural mechanics. The design procedure was based upon the requirements of the current American steel design standards [10,14,15] to ensure the practicality and sufficiency of the connection.

In traditional structural design, the connection would be proportioned after the appropriate beam sections have been selected to resist a given combination of loads. Thus, some properties such as the beam section size and beam material properties were assumed to be determined here,

prior to the connection design. This means that the thickness of the teeth is equal to the beam flange thickness and should not be adjusted when the connection is being designed. Other geometric parameters, such as the length of a single tooth, the number of teeth, and the size of the angles are dependent upon one another and must be chosen iteratively during the design of the connection for moment.

Another basic assumption in this design procedure is that the connection will transfer the moment and shear loads separately; meaning the angles will take all the load due to moment, and the plates will take all the load due to shear. Therefore, the design procedure of side-intermeshed connection combines two different procedures: 'shear design' and 'moment design'. The shear design follows a conventional shear tab design according to the AISC recommendations [10] which results in the selection of suitable shear plates and bolts. Moment design, however, requires several steps and likely multiple iterations due to the more complex load transfer mechanism of the intermeshed segments. The moment design process will be discussed in detail in the following paragraphs.

As mentioned previously, these connections are not recommended for placement near the location where maximum moment will be experienced. Therefore, the full plastic capacity of the beam section is not required to be developed by the connection, and a fraction of this capacity becomes a design choice. In this research, one-third the plastic moment capacity of the beam was selected as the design moment ($M_d$). As previously stated, one of the basic assumptions of this design procedure is that the angles take all the moment load without any contribution from other connection elements. The design moment, $M_d$, transfers through the angles in form of a force couple, i.e. compression in the top angles, $P_d$, and tension in the bottom angles, $T_d$ (assuming positive bending moment). Assuming all four angles and the corresponding flange teeth are

identical, each top angle takes $P_d/2$ and each bottom angle takes $T_d/2$ from the load share. Then, the angles are proportioned at these demand levels for 'yielding at the gross section' as well as 'rupture at the net area' based upon the AISC recommendations [10].

Dimensions for the circular cuts ($R$) at socket corners were chosen so that an adequate amount of stress could be relieved without significantly reducing the angle cross section. Dimension of the sockets in the angles are a function of the teeth sizes plus the considered tolerances, $g_1$ and $g_2$, on top/bottom and left/right side of the teeth respectively, as shown in Fig. 9a. It is important to notice that at this point, the horizontal dimension of the teeth was still unknown (the vertical dimension equals the beam flange), therefore, an initial value must be assumed. This value was later adjusted during the teeth strength design which will be discussed in the following paragraph. The adjusted value would change the socket size and consequently affect the angle design; thus, this design procedure needs several iterations until the sizes converge.

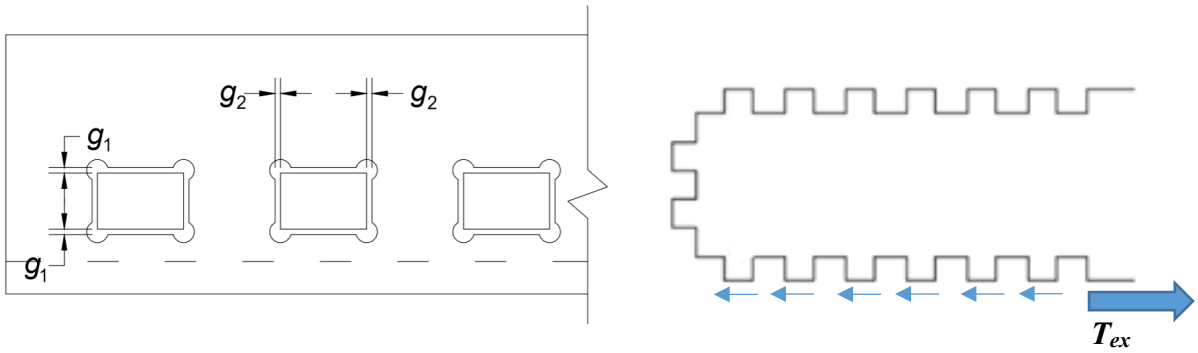


(a) Elevation of teeth and angle (b) Distribution of the load on the tension angle

Fig. 9: Detail of geometry and load path in the connection

In this step of the design, the teeth are sized for the maximum expected forces based on connector angle capacity, which is symbolized as $T_{ex}$ for the tension angle and $P_{ex}$ for the

compression angle. This concept, known as 'Capacity Design', assures that the failure in the angles occurs before the teeth failure. Such mechanism is desirable since the replacement of the angles is easy and fast following any case of damaging overload. Assuming all the teeth have equal contribution in transferring the angle load, each tooth has to bear $T_{ex}/n$ (or $P_{ex}/n$), where $n$ is the number of the teeth on one side of the connection (see Fig. 9b). Therefore, each tooth needs to be checked for the combined shear and moment stresses caused by the external load.

Once all geometries and material properties are stated, the capacity of the connection may be checked against the demand. The size of the connection components may then be increased or decreased to produce an adequate and optimally efficient configuration. Several iterations may be necessary to develop an arrangement that is appropriate for a given moment. The flowchart shown in Fig. 10 helps understand the step-by-step process of the moment design for the side-intermeshed connection.

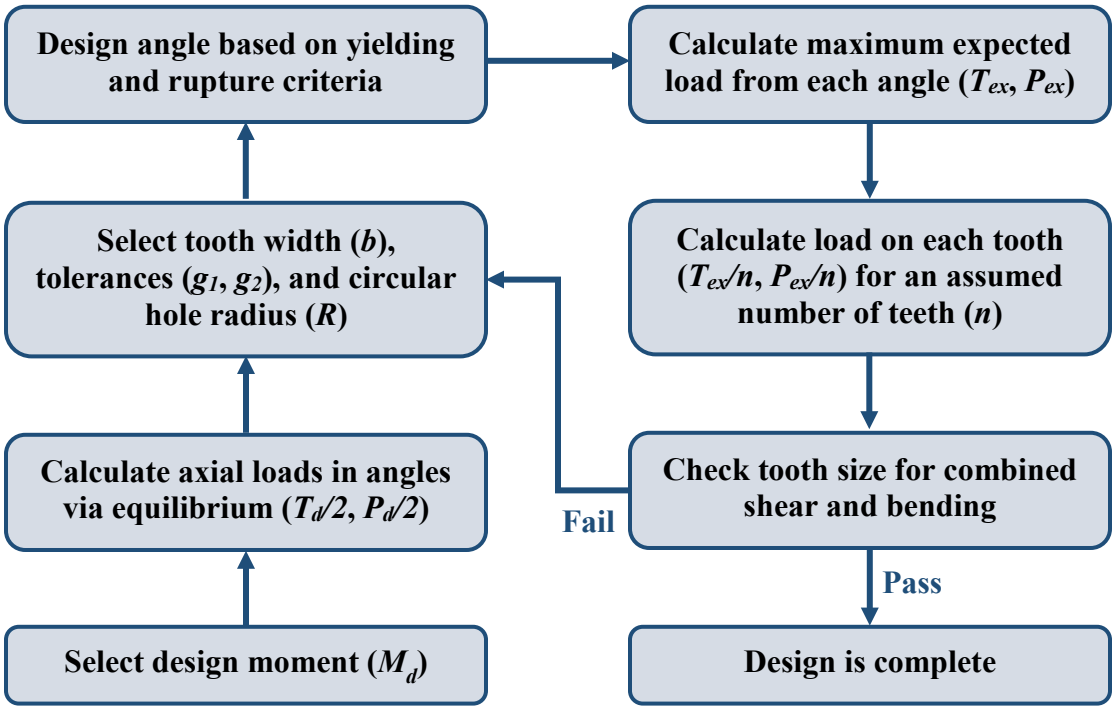

Fig. 10: Moment design of side-intermeshed connection

### 5.2. Fabrication process and challenges

An experimental program at the University of Minnesota aimed to investigate the performance of the side intermeshed connection under different load conditions. For this purpose, two beam sizes, W18x46 and W21x57, were selected from commonly used members based upon engineering judgment. The intermeshed connections were designed for these beams according to the procedure described in the previous section, which resulted in the angle sizes L2½×2×3/8 and L3×2×3/8 respectively.

The side-intermeshed connection was developed primarily to offer greater ease of fabrication and assembly than the front-intermeshed connection. Larger tolerances were included in this configuration to increase the adjustability of the connection, allow connecting elements to be placed safely and easily, and accommodate imperfections in the connected members. A tolerance of 1.6 mm was specified for all the connection components, expect for the circular holes in the angle sockets, which needed a more precise cut of 0.8 mm. These were the precision the cutting machine needed to have in order to meet the project requirements. Furthermore, it had to be able to penetrate the thickest steel element (16.5 mm for the beams and 9.5 mm for the angles), while maintaining the required precision level.

Regarding the precise geometry of the side-intermeshed connection, high-definition plasma and waterjet cutting were selected for manufacturing of different parts based on the project need. Both techniques are capable of cutting structural steel with high precision. Plasma cutting, which works based on a ‘melt and blow’ mechanism, can be used to cut metal plates with the

maximum thickness of 60 mm with 0.25-0.4 mm precision. However, making cuts using plasma is a relatively slow process and the cut finish quality is average. Waterjet cutting, on the other hand, is a very fast technique that provides an excellent smooth cut finish with high precision (0.05-0.2 mm) in 75 mm thickness [16,17]. This technique relies on 'erosion' cutting method which avoids the formation of 'heat affected zone' and keeps the material properties uniformly distributed. Although these advantages make waterjet an attractive cutting technique to use, it is more costly than plasma cutting. Furthermore, it is difficult to integrate waterjet technology into a typical steel fabrication production line [18].

Local and regional fabricators were contacted to investigate the feasibility of fabricating the beams, angles, and shear plates for the side-intermeshed connection. Plasma cutting was selected for the fabrication of the beams and shear plates. The manufacturer used a Python X Robotic CNC (Computer Numerical Control) Plasma Cutting System for their fabrication. The plasma cutting of one of the beam specimens is shown in Fig. 11a. Although plasma cutting could guarantee the precision of 1.6 mm required for the beams, it could not achieve the 0.8-mm precision in the angles sockets. Therefore, waterjet technique was selected to fabricate the angles. The manufacturer used an OMAX A-Jet waterjet cutting machine to cut the angles and successfully reach the specified precision. Another reason for using waterjet cutting for the angles was to prevent heat affected zones to build around the sockets. Large plasticity was expected to occur in the angles and a heat affected zone could cause brittle fracture through a potential change in the material properties. Fig. 11b shows waterjet cutting of one of the angles.

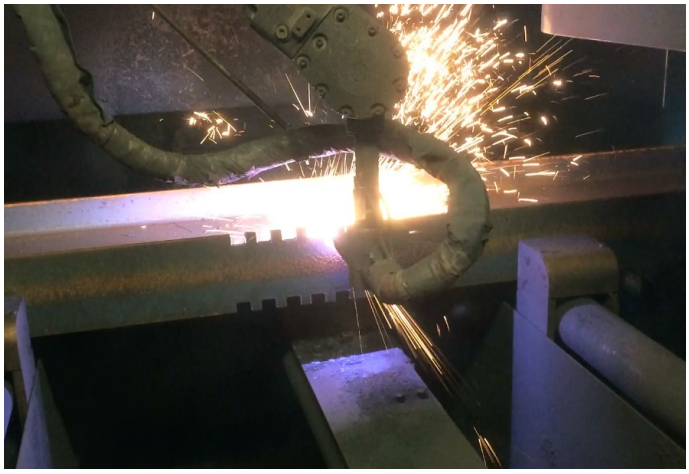

(a) Plasma cutting performed by an industrial robot

(b) Waterjet CNC cutting machine

Fig. 11: Advanced cutting techniques

The required capability to manufacture the specimens was found at steel fabrication shops near the University of Minnesota. The fabricators were able to meet the needs of the projects without significant changes to their fabrication procedures. Once the specimens arrived in the laboratory, they were measured with calipers to check the accuracy of the fabrication. On the beams, every single tooth was measured, and the maximum deviation was found to be 1.4 mm which is within the specified tolerance value of 1.6 mm. Every socket on every angle was also measured. The maximum deviation in both the width and the height of each socket was found to be 0.4 mm which is well within the allowable tolerance value of 0.8 mm. The measurements verified that both plasma cutting and waterjet cutting are acceptable for the precision required for the side-intermeshed connection.

### 5.3. Structural performance - experimental study

Four full-scale beam specimens with intermeshed connection were designed using the design procedure in Section 5.1, and fabricated using precise, fully automated cutting techniques. An experimental testing program was conducted with these specimens to study the behavior of

intermeshed connections under gravity loads. The validity of the proposed design procedure also needed to be verified with experimental testing in order to gain acceptance for adoption by design and construction codes.

The experimental work involved four major-axis beam tests with the intermeshed connection located along the beam span and in two different locations. In the first two specimens, the connection was in the middle of the beam, while in the other two specimens, it was located at the beam end (Fig. 12). This change in location was to study the effect of connection location on the global behavior of the specimen. In the first test, the connection was placed in the pure moment region, whereas in the other three tests, the connection was subjected to a combination of bending moment and shear forces with different ratios (see Table 2). Structural steel used for the beam and angles were Grade 50 and Grade 36, respectively, as specified by the American Society for Testing and Materials (ASTM) [19,20]. The specimens were quickly and easily assembled for each test and required no skilled or time-consuming labor.

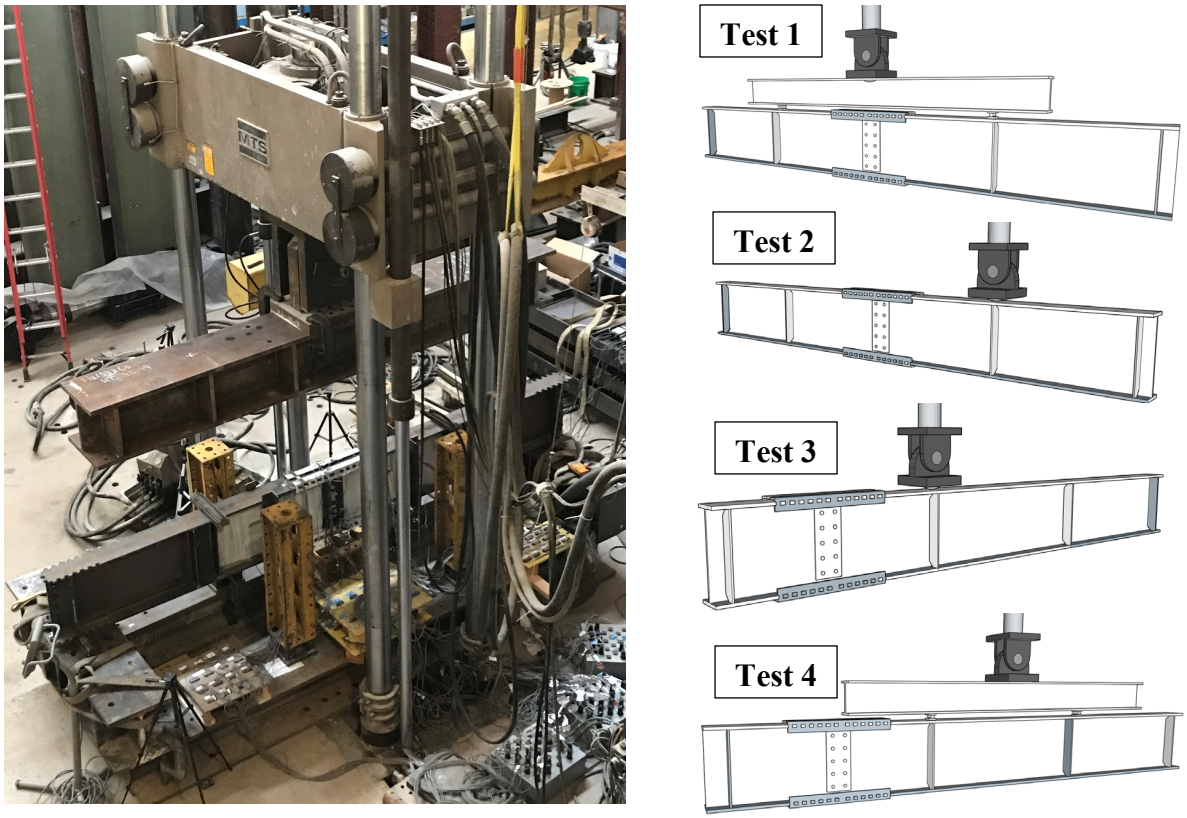


(a) Loading jack and specimen in the laboratory (b) Loading conditions of Test 1 to Test 4

Fig. 12: Test setup

Table 2: Description of test specimens

| Test # | Loading condition | | | Specimen sizes* | |
|---|---|---|---|---|---|
| | Loads at connection | Point Loads | Moment to shear ratio (m) | Beams | Angles |
| 1 | Pure bending | 2 | N.A. | W18×46 | L2½×2×3/8 |
| 2 | Bending plus shear | 1 | 1.84 | W18×46 | L2½×2×3/8 |
| 3 | Bending plus shear | 1 | 0.61 | W21×57 | L3×2×3/8 |
| 4 | Bending plus shear | 2 | 0.61 | W21×57 | L3×2×3/8 |

* US designations for hot rolled steel shapes

Fig. 13 shows the results of all four tests in terms of load-displacement curves, where load was recorded in the loading jack and the vertical displacement was recorded at the connection location. Results showed that, in all cases, the specimens with intermeshed steel connection exhibited ample load carrying capacity and ductility. Table 3 summarizes some of the experimental results in terms of performance criteria such as deformability, capacity, and stiffness. In this table,

the deformability is defined as the ratio of the displacement at the peak load ($\Delta_P$) over the displacement at which the specimen starts yielding ($\Delta_y$). Results show a displacement ratio range of 2.7 to 3.9, which shows the ability of the specimens to undergo significant plastic deformation before reducing peak load. While showing excellent deformability, the specimens exhibited ample load resistance, as the generated loads in the specimens were as high as 0.77 to 0.95 of $M_p$, the plastic moment capacity of the beam sections. This confirms that load could be transferred in the intermeshed steel connection via direct contact of different parts and without using welding or major bolting. Thus, beams with intermeshed steel connections can resist gravity loads expected in typical moment frames.

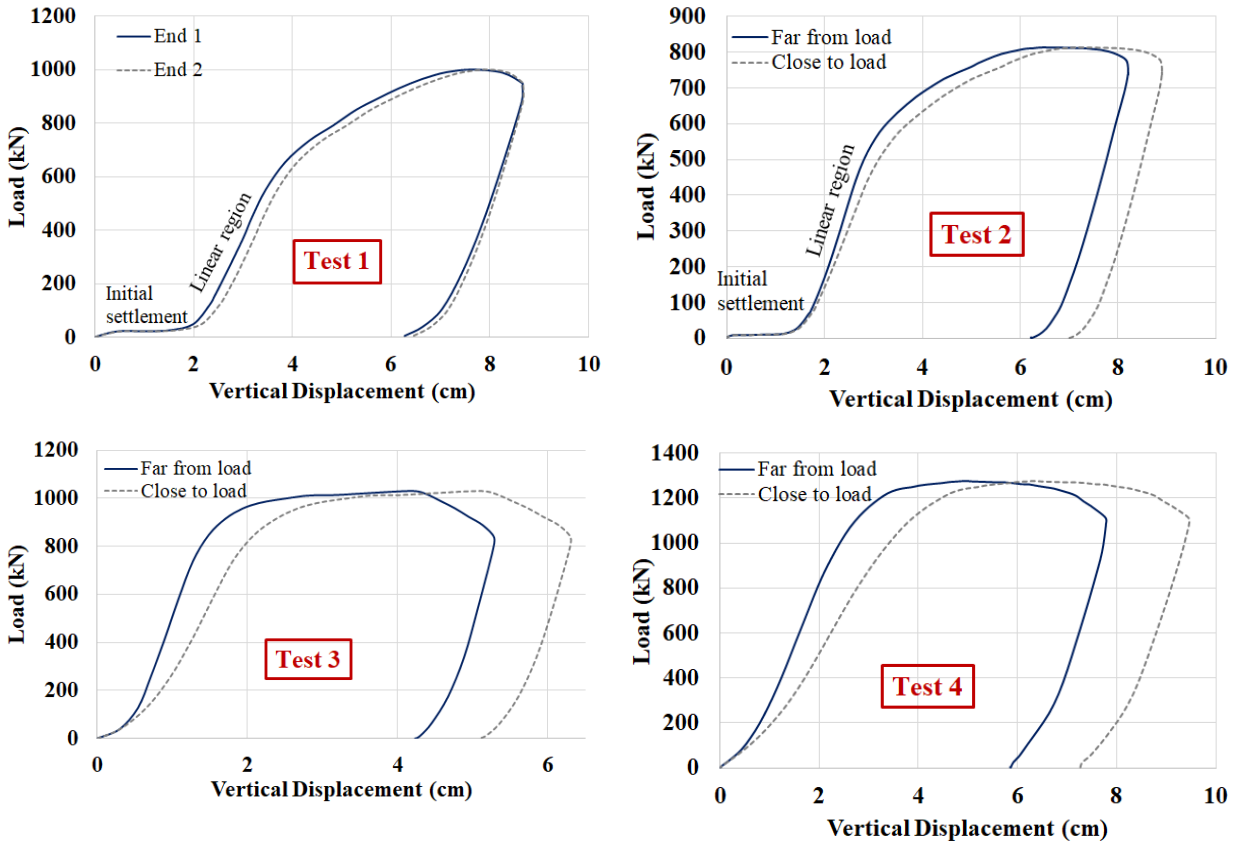


Fig. 13: Load at jack versus vertical displacement at connection ends for Test 1 to Test 4

On the other hand, Table 3 illustrates that the stiffness of the specimens ($K_s$) was a fraction of the stiffness of the corresponding beam without the intermeshed connection ($K_b$). Another words, installation of the intermeshed connection in a continuous steel beam causes a reduction in the elastic stiffness of the beam, which could be as large as 47 to 76 percent. This is due to the discontinuity at the connection region. Although closing the specimen gaps in the loading process helps with stiffness formation, not all gaps will close completely and there will still be some contacts that are not fully stablished. As a result, the intermeshed connection cannot attain the ultimate beam stiffness and it only provides a fraction of that value. This stiffness loss might raise some concerns for the application of the intermeshed system in steel moment frames. However, results of Section 3 of this paper showed that when the intermeshed connection is located away from the beam ends, the reduction in connection stiffness has no major effect on the stress or deflection responses of the frame.

Table 3: Summary of the test results

| Test # | Deformability* ($\Delta_P / \Delta_y$) | Load Capacity ($M_{max} / M_p$) | Initial Stiffness* ($K_s / K_b$) |
|---|---|---|---|
| 1 | 3.8 | 0.77 | 0.50 |
| 2 | 3.9 | 0.94 | 0.53 |
| 3 | 3.3 | 0.95 | 0.45 |
| 4 | 2.7 | 0.88 | 0.24 |

* Not including the 'initial settlement' region of Tests 1 and 2

In all four tests, the specimen started to exhibit out-of-plane movement, and eventually failed due to lateral-torsional buckling. This is because in the late stages of loading, the specimens experienced high plasticity which caused a significant reduction in the material stiffness and subsequently in sectional and member stiffness. Fig. 14 shows the specimens after the test was completed. As can be seen, the out-of-plane failure mode was a product of pure lateral buckling (Test 2 and Test 4) or a combination of lateral and torsional buckling (Test 1 and Test 3). In any case, out-of-plane deflection occurred somewhere between the lateral braces and caused the specimen to lose its load bearing ability. Thus, the bracing design was modified as the program progressed from one test to the next due to the need for additional lateral restraint.

(a) Test 1

(b) Test 2

(c) Test 3 (d) Test 4

Fig. 14: Failure of the specimens due to lateral-torsional buckling

Fig. 13 shows an almost flat initial branch in the load-deflection curves of Tests 1 and 2, which is labeled as 'initial settlement'. During this phase, the first and second specimens, respectively, deflected 2 cm and 1.3 cm under small loads, as a result of the very small stiffness. Visual observations during the tests showed that in this stage of loading, the 'teeth and sockets' were moving towards each other and the 'bolts and shear plates' were slipping towards one another. In fact, the full stiffness of the specimen was not formed until different connection elements came into contact and, subsequently, engaged in the load resistance.

While the initial settlement was relatively large in first two tests, this phenomenon was minimal in Tests 3 and 4, and those specimens began picking up load almost immediately after the test started (see Fig. 13). The reason is that, in the last two tests, the intermeshed connections were placed near the specimen end, and therefore a shorter lever arm was formed. In these specimens, gaps closed faster since the horizontal movement is a function of the lever arm length.

As it is illustrated in Fig. 4b, the intermeshed connection was established based on the premise of being placed at beam ends in a steel moment frame. Therefore, the initial settlement is not a concern for practicality of this system, as it would be small in that configuration. In any case, there exist some practical ways to control the deflections in a frame with intermeshed connections if needed. For instance, some camber could be introduced to eliminate deflections from floor deck weight. Tighter tolerances could also be used in the connection region, as the assembly process definitely showed some leeway in fitting all the connection parts together.

# 6. CONCLUSIONS

This study analyzed a radically new connection for structural steel members, which uses multi-degree of freedom, volumetric cutting to reduce fabrication costs and vastly simplify and speed erection. These fully automated cutting techniques could enhance the fabrication process and consequently increase the productivity of construction. Based on this concept, two different alternatives of intermeshed connection were proposed and investigated via finite element modeling in Abaqus and experimental examination in laboratory.

Results showed that the front-intermeshed connection exhibits excellent shear resistance but axial and flexural behavior are affected by the alignment of the intermeshed flanges. Based on the flexural characteristics of the connection, the front-intermeshed connection shows low stiffness and resistance rendering it a simple connection. For these reasons, this version of the intermeshed connection was not pursued further in this study.

In keeping with the intermeshed connection concept, another alternative is proposed that offers larger load capacity potential and larger erection tolerances. The resulting side-intermeshed connection was designed, fabricated, and tested in the laboratory. Python X Robotic CNC plasma and OMAX A-Jet waterjet cutting machines could successfully meet the required precision of the intermeshed connection, determined in the design process. The results of experimental study on four samples demonstrated high load carrying capacity as well as ample ductility and stiffness. All four specimens failed due to lateral-torsional buckling, even though the lateral restraining system was improved from Test 1 to Test 4. However, in real practice, the lateral-torsional buckling of this system would be of much lesser concern, since the top flanges are usually restrained by a deck.

## 7. ACKNOWLEDGMENTS

The authors gratefully acknowledge the financial support provided by National Science Foundation (NSF) through the grant CMMI-1563115, by Science Foundation Ireland through grant SFI/15/US/B3234, by the Department for the Economy (DfE) and Invest Northern Ireland (InvestNI) through grant USI-096, and by Enterprise Ireland through grant CF20160454. The authors are very grateful to the American Institute for Steel Construction (AISC) for donating the steel beams, angles and plates that were used to build the test specimens. The authors also express their appreciation to the Department of Civil, Environmental, and Geo-Engineering at the University of Minnesota for providing the fourth author (Ramzi Labbane) a departmental fellowship. Lastly, the authors would like to thank Grunau Metals and Am-Tec Designs, the manufacturers that fabricated the beams and angles, respectively.

## 8. REFERENCES

[1] S. Ramakrishnan, M. Gershenzon, F. Polivka, T.N. Kearney, M.W. Rogozinski, Plasma generation for the plasma cutting process, IEEE Trans. PLASMA Sci. 25 (1997) 937–947.

[2] N.D. Perreira, R.B. Fleischman, B. V Viscomi, L.-W. Lu, Automated Construction and ATLSS Connections; Development, Analysis, Experimentation, and Implementation of ATLSS Connections for Automated Construction, 1993.

[3] McKinsey Global Institute, Reinventing Construction: A Route to Higher Productivity, 2017.

[4] D. Krajcarz, Comparison Metal Water Jet Cutting with Laser and Plasma Cutting, Procedia

505 Eng. 69 (2013) 838–843. doi:10.1016/j.proeng.2014.03.061.

506 [5] BOC Linde group, Facts about plasma technology and plasma cutting, 2011.

507 [6] L. Dahil, I. Dahil, A. Karabulut, Comparison of Advanced Cutting Techniques on Hardox
508 500 Steel Material and the Effect of Structural Properties of the Material, Metalurgua. 53
509 (2014) 291–294.

510 [7] S.A. Al Sabah, D.F. Laefer, GB Patent Application No 1718744.4, 2017.

511 [8] P. Matis, T. Martin, P. McGetrick, D. Robinson, The effect of frictional contact properties
512 on intermeshed steel connections, in: Civ. Eng. Res. Irel., Civil Engineering Research in
513 Ireland, Dublin, 2018: pp. 547–553.

514 [9] D. Systems, Abaqus 6.13, (2013).

515 [10] American Institute for Steel Constructions, Specification for Structural Steel Buildings,
516 2016.

517 [11] Eurocode, Eurocode 3: Design of steel structures - Part 1-8: Design of joints, 2005.

518 [12] S.A. Al Sabah, D.F. Laefer, GB Patent Application No 1718746.9, 2017.

519 [13] J. Sikora, A Summary of Stress Concentrations in the Vicinity of Openings in Ship
520 Structures, DAVID W TAYLOR Nav. Sh. Res. Dev. Cent. BETHESDA MD Struct. DEPT.
521 (1973).

522 [14] AISC, Steel Construction Manual, 15th Ed., American Institute of Steel Construction, 2017.

523 [15] American Institute of Steel Construction, Seismic Provisions for Structural Steel Buildings,
524 2016.

525 [16] P. McGetrick, T. Martin, P. Matis, D.F. Laefer, S. Al-Sabah, L. Truong-Hong, M.P. Huynh,
526 A.E. Schultz, J.-L. Le, M.E. Shemshadian, R. Labbane, The AMASS Project: Advanced
527 Manufacturing and Assembly of Steel Structures (submitted), Struct. Build. J. (2019).

528 [17] www.omax.com, Cutting Material with an Abrasive Waterjet, (2019).
529 https://www.omax.com/frequently-asked-questions.

530 [18] S. Al-Sabah, D. Laefer, L. Truong Hong, M.P. Huynh, J.-L. Le, T. Martin, P. Matis, P.
531 McGetrick, M.E. Schultz, Arturo Shemshadian, R. Dizon, Introduction of the Intermeshed
532 Steel Connection - A New Universal Steel Connection (submitted), Build. J. (2019).

533 [19] ASTM, ASTM A992 / A992M: Standard Specification for Structural Steel Shapes, 11
534 (2014) 11–14.

535 [20] ASTM, ASTM A36/A36M - Standard Specification for Carbon Structural Steel, (2018).

536